Article (refereed) - postprint

Detection and attribution of nitrogen runoff trend in China's croplands

Xikang Hou [1,+], Xiaoying Zhan [1,+], Feng Zhou [1,*], Xiaoyuan Yan [2], Baojing Gu [3],

Stefan Reis [4,6], Yali Wu [1], Hongbin Liu [5], Shilong Piao [1], Yanhong Tang [1]

1. Sino-France Institute of Earth Systems Science, Laboratory for Earth Surface
   Processes, College of Urban and Environmental Sciences, Peking University,
   Beijing, 100871, P.R. China

2. State Key Laboratory of Soil and Sustainable Agriculture, Institute of Soil
   Science, Chinese Academy of Sciences, Nanjing, 210008, P.R. China

3. Department of Land Management, Zhejiang University, Hangzhou 310058, P.R.
   China

4. Natural Environment Research Council, Centre for Ecology & Hydrology, Bush
   Estate, Penicuik EH26 0QB, United Kingdom

5. Institute of Agricultural Resources and Regional Planning, Chinese Academy of
   Agricultural Sciences, Beijing 100081, P.R. China

6. University of Exeter Medical School, Knowledge Spa, Truro, TR1 3HD, United
   Kingdom

[+] X.K.H and X.Y.Z contributed equally to this work.

[*] Corresponding author. Phone: +86 10 62756511. Email: zhouf@pku.edu.cn (F. Z.)

23   **Acronyms and Abbreviations**

R_{TN}	Cropland N runoff	RR	R_{TN} per unit N fertilizer additions
R^0	Background N runoff	pH	Soil pH value
SOM	Soil organic matter	$Clay$	Soil clay content
TN	Soil total nitrogen	$Temp$	Mean air temperature
N_{rate}	Nitrogen (N) fertilizer application rate per unit sowing area	W	Sum of precipitation and irrigation within observation period
x_k	Environmental variables	CE	Correction coefficient

24

Abstract

Reliable detection and attribution of changes in nitrogen (N) runoff from croplands are essential for designing efficient, sustainable N management strategies for future. Despite the recognition that excess N runoff poses a risk of aquatic eutrophication, large-scale, spatially detailed N runoff trends and their drivers remain poorly understood in China. Based on data comprising 535 site-years from 100 sites across China's croplands, we developed a data-driven upscaling model and a new simplified attribution approach to detect and attribute N runoff trends during the period of 1990-2012. Our results show that N runoff has increased by 46% for rice paddy fields and 31% for upland areas since 1990. However, we acknowledge that the upscaling model is subject to large uncertainties (20% and 40% as coefficient of variation of N runoff, respectively). At national scale, increased fertilizer application was identified as the most likely driver of the N runoff trend, while decreased irrigation levels offset to some extent the impact of fertilization increases. In southern China, the increasing trend of upland N runoff can be attributed to the growth in N runoff rates. Our results suggested that increased SOM led to the N runoff rate growth for uplands, but led to a decline for rice paddy fields. In combination, these results imply that improving management approaches for both N fertilizer use and irrigation is urgently required for mitigating agricultural N runoff in China.

Keywords: Nitrogen runoff; temporal trend; spatial pattern; attribution analysis; Bayesian inference

Capsule

Cropland N runoff in China increased by 30% over the past two decades mainly due to increased fertilization and decreased irrigation.

Highlights

- A data-driven upscaling model can effectively and reliably detect N runoff trends
- N runoff has increased by 46% for rice paddy fields and 31% for uplands since 1990
- SOM change results in inverse trend of N runoff rates between upland and rice fields

1. Introduction

Meeting food security targets while simultaneously reducing reactive nitrogen losses has drawn attention from both scientists and the public (Chen et al., 2014; Mueller et al., 2012; Tilman et al., 2011; Zhang et al., 2015). Large amounts of anthropogenic nitrogen (N) inputs have resulted in excess N being lost in runoff from croplands to water bodies and the atmosphere worldwide (Cui et al., 2014; Leip et al., 2011; Seitzinger et al., 2010). As one of the consequences, increased occurrences of aquatic eutrophication and ecosystem degradation were observed, particularly in China and South Asia (Paerl et al., 2014). Reliable detection and attribution of cropland N runoff are crucial for policy makers and farmers to develop site-specific N management strategies (Cherry et al., 2008). Although cropland N runoff is substantial in China (e.g., 2.1±0.2 or 0.8 Tg N yr^{-1} estimated by Gu et al., (2015) and Wang et al., (2014), respectively), large-scale, spatially detailed N runoff trends and its attribution remain poorly understood.

Cropland N runoff, defined as a generation process of N loss via surface runoff, depends on environmental conditions and agricultural management practices (Zhang et al., 2016). This complexity makes large-scale N runoff difficult to estimate using empirical models. Plot-scale N runoff flux data from croplands are also difficult to scale up into spatially detailed maps because of spatio-temporally varying results (Shen et al., 2012). Currently, an export coefficient approach has been widely used to estimate cropland N

78   runoff (Hao, 2006; Liu et al., 2010; Velthof et al., 2009; Wang et al., 2014). For example,

79   the first National Pollution Census Program of China (NPCP) provided a collection of

80   N runoff flux coefficients for different geographical regions in China, determined by

81   fitting cross-sectional site data to an export-coefficient model (Wang et al., 2014).

82   Nevertheless, substantial evidence gathered from field observations indicates that linear

83   and homogeneous models are rarely capable of capturing the spatial variability of N

84   runoff at regional scale (Schaefer and Alber, 2007; Sobota et al., 2009; Hou et al., 2016).

85   This highlights the difficulty of accurately predicting its future evolution as well as

86   quantifying the impacts on aquatic ecosystems.

87

88   While it is still challenging to attribute contributions of each individual driving factor

89   (e.g., climate condition, agricultural management practices) to the cropland N runoff

90   trend assessment, statistical correlation or regression analyses have been widely applied

91   (Korsaeth and Eltun, 2000; Stalnacke et al., 2015) over past decades. However, this

92   approach has two potential limitations. Firstly, statistical analyses of historical R_{TN}

93   generally characterizes the related major drivers, thus includes the signals not only from

94   the temporal trends, but also from inter-annual or decadal variability. Secondly, the use

95   of statistical analysis generally assumes that the effects of drivers on N runoff are linear

96   and independent of each other (Piao et al., 2015). However, a growing number of

97   studies based on both data from field experiments and theoretical analyses indicated

98   non-linear responses of N runoff to changes in driving factors as a consequence of

99   complex interactions (Hou et al., 2016). Although these limitations in attribution

100 analysis could be overcome through the application of process-based models (Hao,

101 2006; Abbaspour et al., 2015, Liu et al. 2016), core limitations of such simulation

102 models are the large uncertainties arising from model structure and parameter choice

103 (Schulz et al., 1999). One way to separate the contribution of natural and anthropogenic

104 controls is to use the Kaya Identity concept developed in economics (Raupach et al.,

105 2007), which is adopted when studying climate change and hydrological science

106 (Streimikiene and Balezentis, 2016; Wang et al., 2015b).

107

108 To quantify and attribute cropland N runoff trends during past decades, we analyzed the

109 data in this study is based on a upscaling model following a new simple attribution

110 approach. Synthesized field measurements were used for model calibration and cross-

111 validation based on the Bayesian Recursive Regression Tree algorithm version 2.0

112 (BRRT v2, Zhou et al., 2015), utilizing high-resolution gridded datasets including

113 climate conditions, soil attributes, and agricultural management practices. First, we

114 assessed inter-annual dynamics of cropland N runoff derived from the data-driven

115 upscaling model to detect trends for the period from 1990 to 2012. Second, we

116 compared the proportional change rate of each driver to upscaling results of R_{TN}, which

117 allowed us to diagnose the contributions of different drivers. Finally, we discussed how

118 each driver modulates the temporal trend of R_{TN} and the implications for site-specific

119 N management.

120

2. Data and methodology

2.1 Dataset

Based on the National Pollution Census Program of China (NPCP) and datasets published by the scientific community, *in situ* measurements of N runoff and associated variables in each plot were collated from 100 experimental sites for both rice paddy and upland fields (i.e., as a flooded parcel of arable land used for growing rice and non-rice crops, respectively). Water samples were collected in the drainage outlet for each rainfall event in most of the measurements, where the runoff volume was consecutively measured within the observation period. N concentrations in water samples were analyzed using ultraviolet spectrophotometric methods, following the Standard Methods for the Examination of Water and Wastewater approach for China (SEPA, 2002). Precipitation within the observation period and soil properties (0-20 cm depth) at the beginning of the experiment were synchronously monitored. Missing values of soil properties or climatic factors at a few sites were supplemented with data from the China Soil Scientific Database (http://vdb3.soil.csdb.cn/) based on the corresponding soil type of the county or from the 0.1-degree China Meteorological Forcing Dataset (CMFD) v0106 (http://data.cma.cn/) depending on its geographic coordinates. Information on agricultural management practices including N fertilizer application rate, irrigation amount, fertilizer types, and crop types were recorded, including the timing of the application. The dataset comprised 535 site-years data (293 for upland

141 and 242 for rice paddy fields) (Fig. 1a and Supplementary Data S1), and can be

142 considered representative of most major cropping areas except northwestern China (Fig.

143 1).
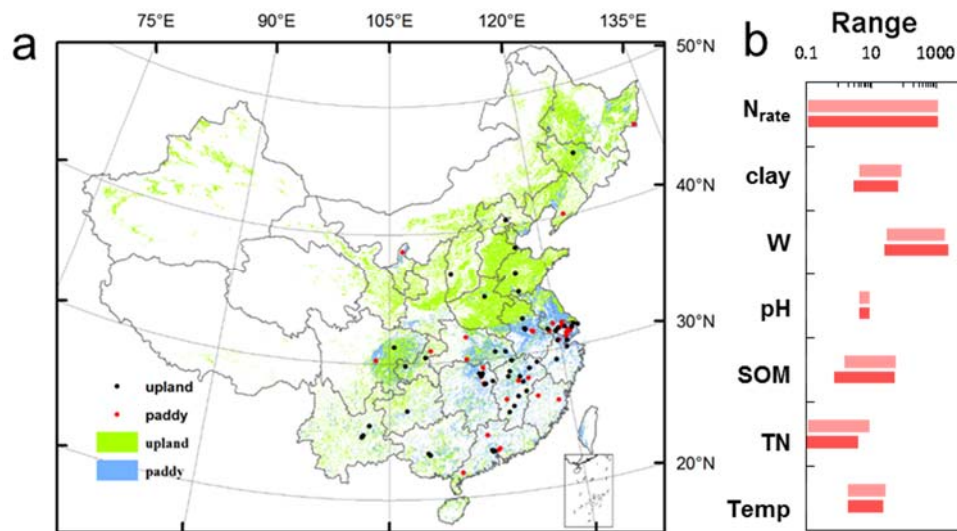
144

145 **Figure 1. Location of experimental sites on cropland N runoff in China.** Sixty-two

146 experimental sites for upland are illustrated as black solid circles, whereas thirty-eight

147 sites for paddy field are indicated as red solid circles. The ranges of each individual

148 variable is illustrated as a light red bar for observational datasets and a dark red bar for

149 croplands for the whole of China in panel b. The variables are N_{rate} (kg N ha^{-1}), clay

150 content (Clay, %), water input (W, mm), soil pH, soil organic matter (SOM, g kg^{-1}),

151 soil TN (g kg^{-1}) and air temperature (Temp, °C).

152

153 **2.2 Data-driven upscaling model**

154 We developed an upscaling model which accounts for the effects of environmental

155 conditions and agricultural management (Eq. 1). Specifically, N fertilizer application

156 rate (N_{rate}) and environmental conditions (x_k) are directly included as independent

157   variables, whereas fertilizer application and crop types are considered as correction

158   terms in the model:

159   $$R_{TNl} = RR_l(x_k) \cdot N_{rate} + R^0_l(x_k) + \varepsilon, \quad \forall l=1,2,\ldots,L, \quad x_k \in \Omega_l \tag{1a}$$

160   where

161   $$RR_l = RR_l^*(x_k) \times CE_i(RR) \times CE_j(RR), \tag{1b}$$

162   $$R^0_l = R_l^{0,*}(x_k) \times CE_j(R^0), \tag{1c}$$

163   $$RR_l^*(x_k) = f(x_k) \cdot N_{rate} + g(x_k), \quad R_l^{0,*}(x_k) = h(x_k), \tag{1d}$$

164   and i and j represent the index of fertilizer types and crop types, respectively; l and L

165   are the index and number of piecewise functions. x_k is climatic condition or soil attribute.

166   Observations (Fig. S1) of air temperature, water input and soil clay content can be used

167   as proxies to reflect the variations of soil temperature and water content within the

168   observation period, respectively. RR^* and $R^{0,*}$ are the reference values when urea is

169   applied and where wheat or rice are cultivated on experimental sites. Both are then

170   adjusted to reflect different fertilizer and crop types to develop a specific RR and R^0 for

171   a given scenario. The details of correction coefficients (CEs) can be found in Table S1.

172   It should be noted that fertilizer types considered include urea, compound fertilizers,

173   manure and/or crop residues, and ammonium bicarbonate. In addition, crop types

174   distinguish between rice, wheat, maize, soybean, cotton, and other corps.

175

176   The Bayesian Recursive Regression Tree version 2 (Zhou et al., 2015), was

177   subsequently used with observational data to determine optimal L, $f(x_k)$, $g(x_k)$, and $h(x_k)$.

178   The detailed methodological approach of the BRRT v2 is described by Zhou et al. (2015)

179 and Text S2 in the Suppl. Mat.. The resulting calibrated model was applied to simulate

180 spatial patterns of N runoff over Chinese croplands from 1990 to 2012 at a spatial

181 resolution of 1 km. The details on input data used in this model, including N_{rate} by

182 fertilizer and crop types, water input, clay content, air temperature, soil pH, soil organic

183 matter (SOM), and soil N, are described in Table S2 and Fig. S2. Due to the lack of

184 detailed information on the spatio-temporal changes in fertilization methods, timing,

185 and cultivation practices in China, this information was not included in the data-driven

186 upscaling model simulation presented here.

187

188 **2.3 Structural decomposition analysis**

189 We further applied a simplified attribution approach, 'Runoff Identity' (analogous to

190 the Kaya Identity in economics), to assess the contribution of water input changes (W,

191 the sum of precipitation and irrigation amounts), the fertilizer-to-water ratio (the ratio

192 of fertilizer used to water input) and N runoff rate (i.e., the ratio of annual N runoff flux

193 to fertilizer addition) to the relative rate of change of R_{TN} in China. The Runoff Identity

194 combines the variables of regional averaged water inputs and fertilizer addition in a

195 causal relationship to cropland N runoff (R_{TN}). R_{TN} is therefore regarded as the

196 integration of the three variables:

197
$$R_{TN} = W\left(\frac{N_{rate}}{W}\right)\left(\frac{R_{TN}}{N_{rate}}\right) = w \cdot f \cdot e \qquad (2)$$

198 We then defined the proportional change rate of a quantity $X(t)$ as $r(X)=X^{-1}\mathrm{d}X/\mathrm{d}t$ (with

199 units [time]$^{-1}$). Because $((\mathrm{d}R_{TN}/\mathrm{d}t)/R_{TN}) = ((\mathrm{d}R_{TN}/\mathrm{d}t)/(wfe))= ((\mathrm{d}w/\mathrm{d}t)/w) + ((\mathrm{d}f/\mathrm{d}t)/f) +$

200     $((de/dt)/e)$, the Runoff Identity for proportional change rate can be rewritten as

201     $$r(R_{TN}) = r(w) + r(f) + r(e) \qquad (3)$$

202   Using time-series data of w, f and e, we applied this approach to quantify the role of

203   each driver in relation to changes of the R_{TN} trend. The theoretical proportional change

204   rate, which was a sum of factors w, f and e, closely approximates the rate of R_{TN} that

205   actually occurred. We calculate their rates of change over the whole period from 1990

206   to 2012 using a linear regression method, and normalized them by corresponding mean

207   values, respectively. The relative contribution of each factor is the ratio of its

208   proportional change rate to the proportional change rate of R_{TN} during the same period.

209

210   **3. Results**

211   **3.1 Model performance**

212   The data-driven upscaling model (Table S3) was evaluated by reviewing the coefficient

213   of determination (R^2) and coefficient of variation (CV, calculated as the ratio of root-

214   mean-squared error to mean value), which were 0.85 and 39% for rice paddy fields

215   (n=242, Fig. 2a), and 0.85 and 50% for upland grain crops (n=293, Fig. 2b), respectively.

216   The evaluation results suggest that most of the variance of R_{TN} could be explained by

217   the model with acceptable bias. Model performance for R_{TN} per unit N fertilizer

218   additions (RR) ($R^2 = 0.71$ and n=75 for rice paddy fields, Fig. 2c; $R^2 = 0.40$ and n =

219   146 for uplands, Fig. 2d) further indicate that our model is able to capture the sensitivity

220   of R_{TN} to N inputs. Regionally, there are no evident differences in model performance

221 of R_{TN} across the 7 regions (Fig. 2), but *RR* simulated by our model shows differences

222 compared to observations in East China in particular. Additionally, a few simulated *RR*

223 were different from the observations (Fig. 2), mainly due to the lack of spatially detailed

224 data on specific fertilization methods, cultivation practices, or rainfall intensity in our

225 models (Liu et al., 2016; Miyazato et al., 2010; Wang et al., 2015a; Xu et al., 2013).
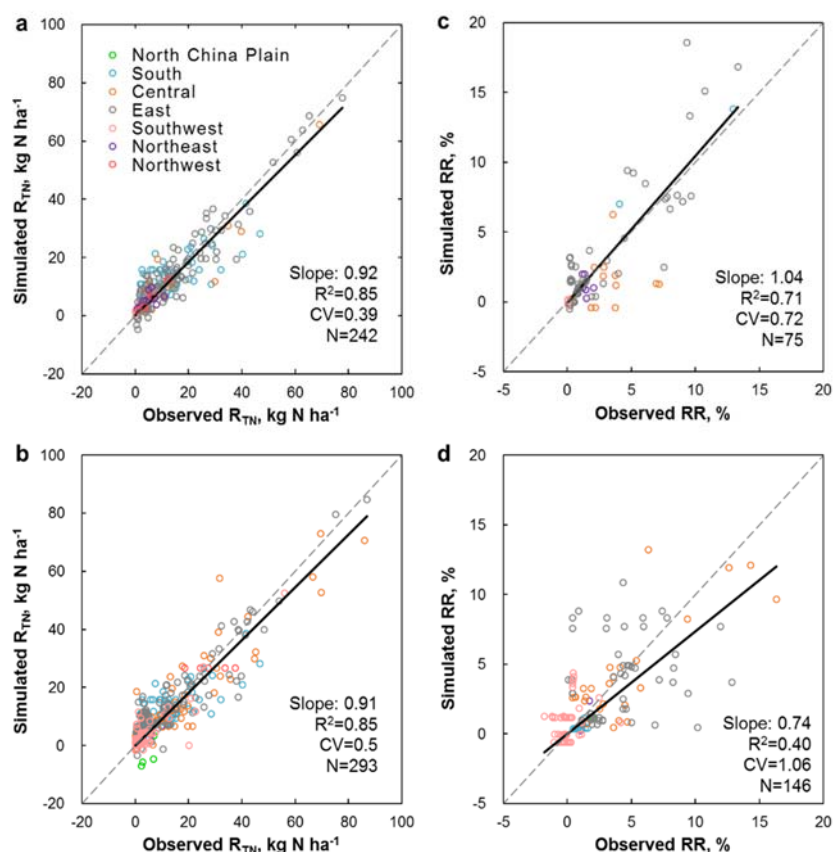
226

227 **Figure 2. Calibration of R_{TN}, RR for paddy fields (panels a and c) and upland**

228 **(panels b and d).** The slope, R^2, and coefficient of variation (CV) are indicated in the

229 insets at the bottom right of each panel. Dots are colored in Fig. 2 to indicate model

230 performances in different regions in China.

231

3.2 N runoff trends and their spatial patterns

Figures 3a and 3b show the annual N runoff or runoff rate from China's rice paddy and upland soils from 1990 to 2012, respectively. In 1990, R_{TN} was 1.69 ± 0.80 Tg N yr^{-1} in China (σ is the standard deviation of N runoff due to the uncertainties of input data and model parameters), splitting into 0.46 ± 0.08 Tg N yr^{-1} for paddy field and 1.23 ± 0.51 Tg N yr^{-1} for upland (Fig. 3). More details of uncertainty estimation approach using Monte Carlo ensemble simulations can be found in Text S3. R_{TN} had increased by 2012 by $46 \pm 11\%$ for rice paddy fields and $31 \pm 14\%$ for uplands (σ is the standard deviation of N runoff changes occurring over a 23-year period; Fig. 3a and 3b).
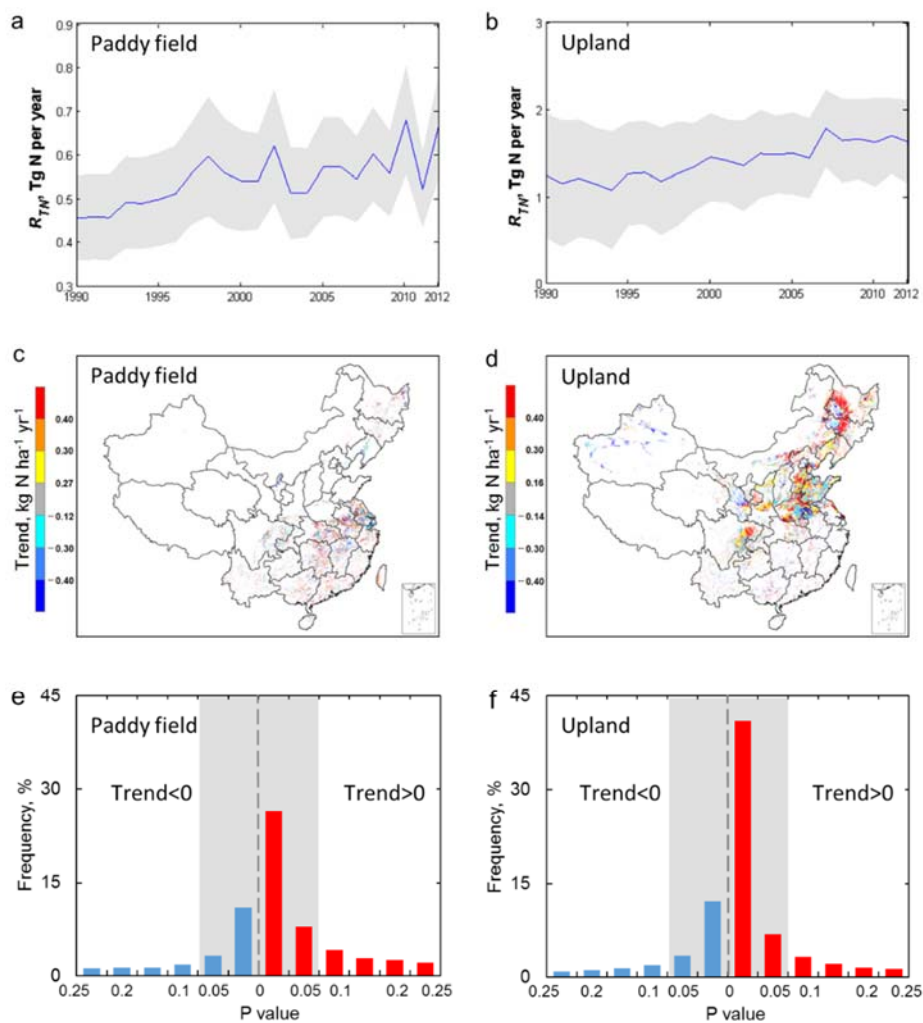
242 **Figure 3**. **Temporal trend of cropland N runoff during 1990-2012.** (a) paddy field;

243 (b) upland; (c) spatial pattern of N runoff trend for paddy field; (d) the same as for c but

244 for upland; (e) frequency distribution of the significance level (P-value) of N runoff

245 trend for paddy field; (f) the same as for e but for upland. The P -value of N runoff

246 trends for each pixel is estimated based on T test. The gray shaded areas in panels (a)

247 and (b) reflect standard deviations based on uncertainty assessments (see Text S2).

248

249 Spatial patterns of the N runoff trends across China for the period from 1990 to 2012

250 were for the land area of China by applying the upscaling model are displayed in Figs.

251 3c and 3d. Both simulation results for rice paddy fields and uplands consistently showed

252 that N runoff trend increased in most regions of China ($P < 0.01$ according to the Mann–

253 Kendall test), while the magnitude of the R_{TN} trend varied for different croplands in

254 China. For rice paddy soils, regions with the largest R_{TN} trend are generally found in

255 southern China and parts of northeastern China (i.e., Amour-Ussuri-Songhua River

256 Plain, defined in Fig. S3), where the trend of R_{TN} is generally larger than 0.4 kg N ha^{-1}

257 yr^{-2}. However, regions that experienced a decreasing trend (14% of croplands) were

258 located in the lower reaches of the Yangtze River Basin, Ningxia Plain, and part of the

259 Sichuan Basin (Fig. S3), where the trend of R_{TN} is –0.12 kg N ha^{-1} yr^{-2}. For uplands,

260 the highest values of the R_{TN} trend (>0.4 kg N ha^{-1} yr^{-2}) are found in northeast China,

261 the Guanzhong Plain, and parts of the North China Plain and Sichuan Basin. In contrast,

262 regions with a decreasing R_{TN} trend (16% of croplands) include the Shandong Peninsula,

263   upper reaches of the Huaihe River Basin, and northwest China (-0.14 kg N ha^{-1} yr^{-2}).

264   The R$_{TN}$ trend is statistically insignificant (P>0.05) in less than 40% of croplands,

265   mainly in the Yangtze River Basin, Shandong Peninsula and Shanxi province (Fig. 3e

266   and 3f).

267

268   **3.3 Attribution of N runoff trends at national scale**

269   For rice paddy fields (Fig. 4a), the relative rate of change of R$_{TN}$ at national scale was

270   1.2 % yr^{-1} over the last 23 years, which was primarily driven by a growing fertilizer-

271   to-water ratio, but partly offset by the decline of water input (28%). For upland, the

272   trend of R$_{TN}$ also showed an increase (1.9% yr^{-1}; Fig. 4b) during the period 1990-2012,

273   with the largest attributable contribution of fertilizer-to-water ratio and a positive

274   proportional change rate of 2.4 % yr^{-1} which was partially offset by the decreased water

275   input (-0.5 % yr^{-1}). Fig. 4 also illustrates the trend of each identity for rice paddy fields

276   and uplands during different periods. The relative R$_{TN}$ change rate for rice paddy field

277   was 2.4 % yr^{-1} prior to the year 2000, but gradually reduced to 1.4 % yr^{-1} during the

278   period of 1990-2005 and then less than 1.2 % yr^{-1} during 1990-2012, primarily due to

279   the decreased growth rate of fertilizer-to-water ratio (3.0 to 1.5% yr^{-1}). However, the

280   trend of R$_{TN}$ for uplands increased from 0.15 % yr^{-1} before 2000 to 0.19 % yr^{-1} during

281   the whole period. This could primarily be explained by the fact that the decrease of

282   growing fertilizer-to-water ratio (from 2.9 to 2.4 % yr^{-1}) was totally offset by the change

283   in the N runoff rate (from -0.9 to 0.01 % yr^{-1}).

284
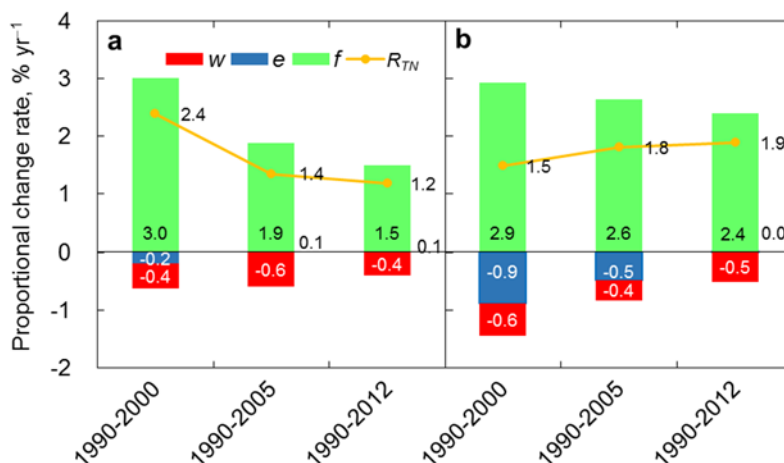
Figure 4. Proportional change rate of cropland N runoff and its drivers. (a) Paddy field; (b) upland. Contributions of the N runoff identity factors during the years 1990-2000, 1990-2005 and 1990-2012, including the water input of precipitation and irrigation (*w*), N runoff rate (*e*) and fertilizer-to-water ratio (*f*).

3.4 Spatial patterns of N runoff trend attributed to different drivers

As demonstrated in Fig. 5, the contributions from three main driving factors to the trend of R_{TN} were highly spatially heterogeneous across different provinces. For rice paddy fields, fertilizer-to-water ratio was the dominant factor for R_{TN} trends in most regions in China, whereas N runoff rate and water input could be attributed to drive the trends in N runoff in eastern coastal regions, and Weihe River Basin (inset plot of Fig. 5a). More specifically, fertilizer-to-water ratio factor alone increased N runoff at a rate of $1.14 \pm 1.05 \%$ yr^{-1} in most rice-cropping areas in southeastern China (Fig. 5a) while N runoff rate had a positive effect on the R_{TN} trend in most regions in southern China at an average of change rate of $1.32 \pm 0.98\%$ yr^{-1}. However, N runoff rate had a more

substantial negative effect on the R_{TN} trend in the other regions and the average trend

of R_{TN} attributed to N runoff rate is -1.12 ± 1.07 % yr^{-1}. In contrast to those two driving

factors, the relative contribution of water input to the R_{TN} trend was minor, but remained

consistently negative for rice paddy fields across the whole country (<-0.14 % yr^{-1}),

except for Taiwan (1.06 % yr^{-1}), Shaanxi (0.99 % yr^{-1}), and Ningxia provinces (0.31 %

yr^{-1}).
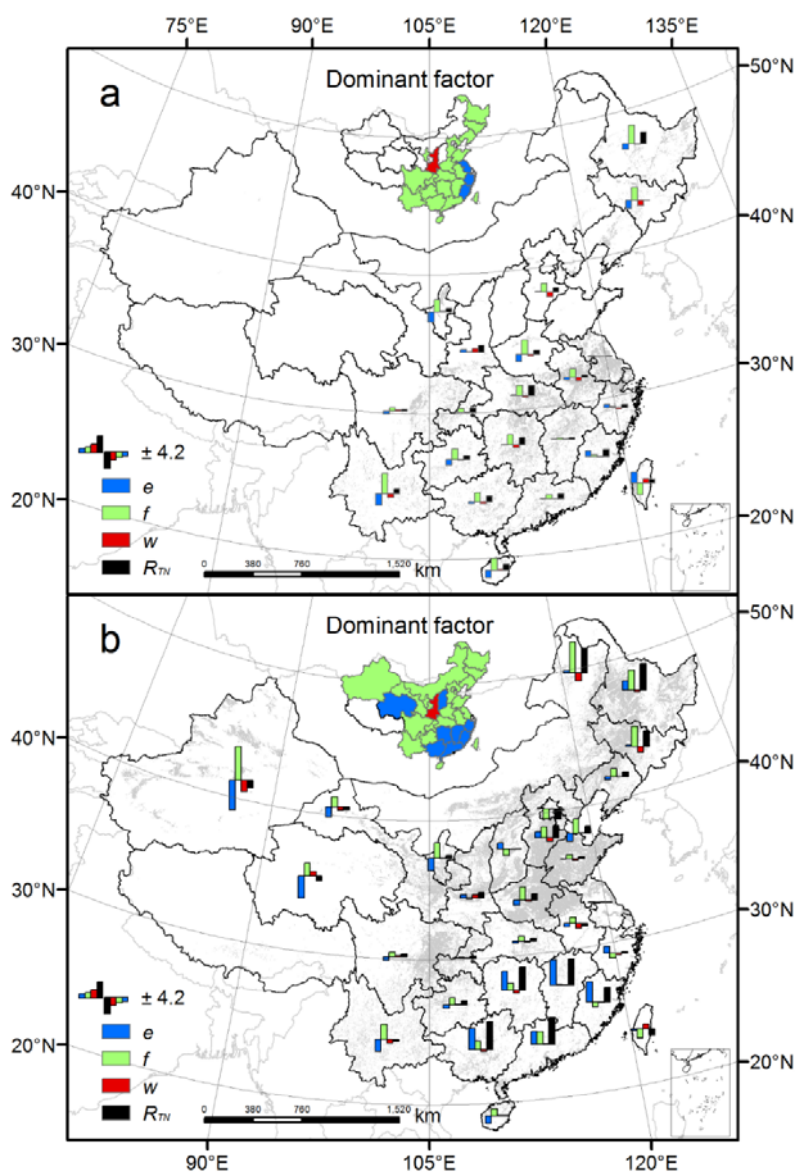
Figure 5. Trends in N runoff and its drivers during the period 1990-2012 at

provincial scale. (a) Paddy fields; (b) upland. The dominant driving factors for the R_{TN}

trend in each province are shown in the insets above the maps. The grey area shows the

spatial pattern of upland or paddy fields in China.

Fertilizer-to-water ratio contributed more to the R_{TN} trend for uplands than for rice

paddy fields in the North China Plain and northeast Plain only. A positive effect of

fertilizer-to-water ratio on the R_{TN} trend was largely offset by N runoff rate changes

across southern China and western China, where the trends of R_{TN} attributed to N runoff

rate averaged at 4.36 ± 1.67 % yr^{-1} and -3.08 ± 2.40 % yr^{-1}, respectively. On the other

hand, the model estimates indicate that N runoff rate changes may result in R_{TN}

increases in southern China (except for Hainan and Taiwan), which were one-fold

higher than the negative effect found across most of northern China. Although there

was no apparent difference in spatial patterns as to water input trends between upland

and paddy field (Fig. 5), the relative contribution of water input to the R_{TN} trend for

upland was less than that for paddy field. In contrast to other regions, water input in

Shaanxi, Taiwan and Hainan provinces has significantly increase ($P < 0.01$). The

increase in trend of R_{TN} due to water input change in Shanxi was larger than due to N

runoff rate and fertilizer-to-water ratio for both crop types. The observations in Taiwan

and Qinghai show that water input change played an important role in R_{TN} increase,

albeit less than the other two driving factors, accounting for 1.2 % yr^{-1} and 1.1 % yr^{-1}

of the trend of R_{TN}. In summary, the effects of agricultural management practices,

including fertilization and irrigation schemes, outweigh the influence of current climate

331 change on model-derived R_{TN} trend increase for both paddy field and upland.

332

333 **4. Discussion**

334 Our findings generally agree well with most prior works, with a few exceptions. For

335 example, Gu et al. (2015) applied an integrated N budget model to constrain the

336 magnitude and trend of N runoff from China's croplands, with an estimate of R_{TN} of

337 2.1 ± 0.2 Tg yr^{-1} with a relative change rate of 1.8 % yr^{-1} during the period 1990-2010.

338 In our study, we explicitly incorporated the non-linear and spatially varied responses of

339 an R_{TN} model at multiple N input levels and reached very similar estimates of total N

340 runoff (1.7 ± 0.2 Tg yr^{-1}) and trend (1.7 % yr^{-1}) while explicitly accounting for spatial

341 variability during the same period (Fig. S4). In addition, Ti and Yan (2013) indicated

342 that the fertilizer-induced N runoff in the Huanghe River Basin, the Yangtze River Basin,

343 and the Paerl River Basin was 1.06 Tg yr^{-1} in 2010 with a relative change rate of 1.4 %

344 yr^{-1} during the period from 1990-2010, which is also comparable to our results (0.72

345 Tg yr^{-1} in 2010 and 1.7 % yr^{-1}). In general, using a new data-driven upscaling model,

346 our estimates derived from a large network of cropland N runoff observations, provide

347 novel insights into the spatially detailed N runoff trend for China's croplands.

348

349 By developing a novel structured decomposition approach for a 'Runoff Identity' (see

350 section 2.3), we are able to accurately identify and quantify the contribution from each

351 individual driver including climatic and human-induced variables to R_{TN} trend. Our

352　results suggest that fertilization (or fertilizer-to-water ratio) is the dominant driver of

353　R_{TN} trends for both rice paddy fields and uplands across most of the country, which is

354　consistent with experimental results at multiple N input levels (Liang et al., 2005; Shi

355　et al., 2010; Yu, 2011). Indeed, over the last two decades, China experienced a growth

356　rate in N fertilizer application of more than 4.0 kg N ha^{-1} yr^{-1} on average in response

357　to a continuous increase in crop production (Fig. S5a). Previous studies suggest that

358　this high rate of N additions to agricultural systems resulted in an increase in soil

359　residual N (Yan et al., 2014). Such accumulated residual N was eventually transferred

360　into aquatic ecosystems (Rasouli et al., 2014). Conversely, eastern and southern coastal

361　regions in Mainland China remained largely unchanged with regard to N application

362　rates and even rates even decreased in Taiwan (Fig. S5a). The N runoff rate in these

363　regions therefore becomes the primary driving force for R_{TN} trends.

364

365　Likewise, we quantified the contribution of water input to the R_{TN} trend increase in

366　China. For rice paddy fields, our model suggests that the decreasing water input offsets

367　27% of the impact of fertilization on the increasing R_{TN} trend at the national scale, and

368　this offset effect is more clearly observed in northern China than in south (Fig. 5).

369　Previous studies indicated that R_{TN} tends to increase with water input (Gao et al., 2016;

370　Hou et al., 2016), because high precipitation and irrigation events in turn resulted in

371　large runoff pulses (Sorooshian et al., 2014). As we illustrated, the decline in water

372　input mainly occurred due to the decrease in irrigation inputs, rather than a marked

373   change in precipitation patterns, except in Taiwan, Hainan and parts of northwestern

374   China (Fig. S6a). Improving the irrigation efficiency could be an effective measure to

375   reduce the overall amount of water used for irrigation in most provinces, whereas the

376   expansion of irrigated area dominates the growth of irrigation mainly in the Northeast

377   Plain, Sichuan Basin, and Yunnan-Guizhou Plateau. Similar drivers and patterns of

378   irrigation trends are found for upland all over the country (Fig. S6b). It should be noted

379   that our per-area irrigation dataset was compiled based on total values at municipal

380   level, rather than on crop-specific amounts (Fig. S5b). Therefore, it would be valuable

381   if future research focused on surveys to address this issue by gathering data per-area

382   irrigation among different crops in each municipal area.

383

384   Our results attributing the contribution by different factors also indicate that the N

385   runoff rate positively affected the R_{TN} trend for uplands across most of southern China,

386   but in general had a negative effect for rice paddy fields (Fig. 5). To interpret such

387   distinct effects on N runoff rates, we conducted two types of scenario assessments to

388   separate the impact of changes in environmental conditions or agricultural management

389   practices: a control simulation with all conditions and practices varying from 1990 to

390   2012 and an experimental simulation with one condition or practice fixed at year 1990

391   levels. The difference was considered as the response to one change in conditions or

392   practices. SOM was identified as the dominant factor for the trends of N runoff rate for

393   both uplands and rice paddy fields nationwide, followed by N_{rate} and water input (Fig.

394   S7). Increased SOM led to N runoff rate growth for uplands, but a decline for rice paddy

395   fields at provincial level during the period1990-2012 (Fig. S8). This result was also

396   confirmed by observations from 63 field sites across China (Fig. S9), and could be

397   explained by the difference in the generation process of N runoff. Upland N runoff

398   begins when raindrops hit the ground and detach soil particles by splash. The sediments

399   eroded from upland fields carry adsorbed N that is subsequently transported

400   downstream. Therefore, high SOM may increase the risk of upland N runoff during

401   rainfall events (Liu et al., 2014). In contrast, N runoff from paddy fields increases when

402   rainfall input exceeds its storage capacity. Overflow through the paddy field levee

403   carries dissolved N into ponding water and rainfall-driven interstitial runoff of nitrate

404   at the soil-water interface to the surrounding water bodies (Huang et al., 2014;

405   Higashino and Stefan, 2014). High SOM improves the adsorption of soil N in ponding

406   water thus lowers the magnitude of N runoff from paddy fields. Additionally, high SOM

407   benefits upland N mineralization under aerobic environment, resulting in increases in

408   soil inorganic N availability and hence N runoff. Little inorganic N, however, will be

409   released from SOM in paddy field under anaerobic environment, which helps reducing

410   N runoff (Wu et al., 2017).

411

412   In this study, we comprehensively quantified and analyzed the attribution factors for N

413   runoff trends in China's croplands. However, we found that some results for simulated

414   N runoff were significantly different from observations (Fig. 2). Previous experiments

415   showed that N runoff or N runoff rate were also changed following different fertilization

416   (e.g., methods, timing), irrigation schemes, or rainfall intensity (Liu et al., 2016;

417   Miyazato et al., 2010; Wang et al., 2015a; Xu et al., 2013). For example, field trials

418   highlighted that the application of controlled release N fertilizers significantly reduced

419   N runoff by 48-72% compared to top-dressing fertilization for paddy fields. Similarly,

420   the application of optimized irrigation methods significantly reduced N runoff by 24%

421   compared to flooding irrigation (Yang et al., 2015); N runoff from paddy fields was not

422   only passively generated by monsoon rain in China, but also a consequence of human-

423   induced drainage before transplanting (Yan et al., 2016). However, the current

424   upscaling model did not fully consider such management practices. Meanwhile, air

425   temperature and clay content were used in this study as proxies for soil temperature and

426   soil water content within the experimental period, respectively, due to the lack of long-

427   term observations across China. Although previous works have found a significant

428   linear relationship between air and soil temperatures or between clay and water contents

429   (Zheng et al., 1993; Wäldchen et al., 2012), more robust estimations of soil temperature

430   and water content become another question to be undertaken by future studies. In

431   addition, *in situ* measurements of N runoff are scarce in Northwest China (e.g., Xinjiang

432   province), leading to large uncertainty in R_{TN} estimates in this regions. Previous studies

433   indicated that the dominant pathways of N losses would be ammonia volatilization to

434   the atmosphere and N leaching to aquifers (Gao et al., 2016; Van Damme et al., 2017),

435   rather than surface N runoff. More importantly, this region accounts for only 8.6% of

436   N fertilizer application and 11% of the sowing area in China and has a low N runoff

437   rate observed in the NPCP (0. 34 $\pm$ 0.26 %). Therefore, N runoff in Northwest China

438   makes a small overall contribution to the total N runoff of Chinese croplands. To

439   confirm the contribution from Northwest China, more observations should be

440   conducted in the future to verify R_{TN} estimates. Furthermore, data from field

441   manipulation experiments on the response of R_{TN} to environmental conditions (e.g.,

442   SOM) is lacking and would be useful to constrain our upscaling model. Therefore,

443   further efforts to make widespread measurements and to carry out field manipulation

444   experiments for R_{TN} are necessary to improve the reliability of such model simulations.

445

446   In summary, cropland N runoff has been increasing significantly in China for the period

447   1990-2012. At a national scale, increases in fertilizer application and decreases in

448   irrigation amounts were identified as the most likely causes for the N runoff trend. The

449   positive contribution of N runoff rate to the R_{TN} trend is more evident in southern China

450   than in the north. We expect a continuously decreasing trend in irrigation amounts into

451   the future, and fertilizer application rates likely to plateau, since China aims to improve

452   water use as well as fertilizer N application efficiencies through the action plans like

453   clean water and "zero-increase fertilizer use" (Ju et al., 2016). However, current

454   projections on climate change suggest that precipitation, particularly extreme rainfall

455   events, will increase. This might further lead to N runoff and N runoff rate increase in

456   the future. In addition to the expected improvements on N use efficiency and water use

457 efficiency in China's croplands, applying effective management approaches that

458 generate benefits for both N runoff and crop yields are urgently required to design more

459 efficient and sustainable agricultural N management. Improving the representations

460 associated with the effects of agricultural management practices and understanding the

461 response of N runoff to environmental conditions should be the priorities for the

462 agricultural modeling.

Acknowledgements

Appendix A. Supplementary data

471 Supplementary information related to this article can be found online, including

472 Supplementary Data S1, Text S1 to S3, Tables S1 to S4, and Figures S1 to S9.

References

474 Abbaspour, K.C., Rouholahnejad, E., Vaghefi, S., Srinivasan, R., Yang, H., Klove, B.,

475 2015. A continental-scale hydrology and water quality model for Europe:

476   Calibration and uncertainty of a high-resolution large-scale SWAT model. Journal

477   of Hydrology 524, 733-752.

478   Chen, X., Cui, Z., Fan, M., Vitousek, P., Zhao, M., Ma, W., Wang, Z., Zhang, W., Yan,

479   X., Yang, J., Deng, X., Gao, Q., Zhang, Q., Guo, S., Ren, J., Li, S., Ye, Y., Wang,

480   Z., Huang, J., Tang, Q., Sun, Y., Peng, X., Zhang, J., He, M., Zhu, Y., Xue, J., Wang,

481   G., Wu, L., An, N., Wu, L., Ma, L., Zhang, W., Zhang, F., 2014. Producing more

482   grain with lower environmental costs. Nature 514, 486-489.

483   Cherry, K.A., Shepherd, M., Withers, P.J., Mooney, S.J., 2008. Assessing the

484   effectiveness of actions to mitigate nutrient loss from agriculture: a review of

485   methods. Science of the Total Environment 406, 1-23.

486   Cui, Z., Wang, G., Yue, S., Wu, L., Zhang, W., Zhang, F., Chen, X., 2014. Closing the

487   N-Use efficiency gap to achieve food and environmental security. Environmental

488   Science & Technology 48, 5780-5787.

489   Gao, S., Xu, P., Zhou, F., Yang, H., Zheng, C., Cao, W., Tao, S., Piao, S., Zhao, Y., Ji,

490   X., Shang, Z., Chen, M., 2016. Quantifying nitrogen leaching response to fertilizer

491   additions in China's cropland. Environmental Pollution 211, 241-251.

492   Gu, B., Ju, X., Chang, J., Ge, Y., Vitousek, P.M., 2015. Integrated reactive nitrogen

493   budgets and future trends in China. Proceedings of the National Academy of

494   Sciences 112, 8792-8797.

495   Hao, F.H., Yang, S.T., Cheng, H.G., Bu, Q.Y., Zheng, L.F., 2006. A method for

496   estimation of non - point source pollution load in the large - scale basins of China

497   (in Chinese). Acta Scientiae Circumstantiae 26, 375 - 383

498   Harrison, J.A., Seitzinger, S.P., Bouwman, A.F., Caraco, N.F., Beusen, A.H.W.,

499   Vorosmarty, C.J., 2005. Dissolved inorganic phosphorus export to the coastal zone:

500   Results from a spatially explicit, global model. Global Biogeochemical Cycles 19,

501   367-384.

502   Higashino, M., Stefan, H.G., 2014. Modeling the effect of rainfall intensity on soil-

503   water nutrient exchange in flooded rice paddies and implications for nitrate

504   fertilizer runoff to the Oita River in Japan. Water Resources Research 50, 8611-

505   8624.

506   Hou, X.K., Zhou, F., Leip, A., Fu, B.J., Yang, H., Chen, Y., Gao, S.S., Shang, Z.Y., Ma,

507   L.K., 2016. Spatial patterns of nitrogen runoff from Chinese paddy fields.

508   Agriculture, Ecosystems & Environment 231, 246-254.

509   Huang, H., Ouyang, W., Guo, B., Shi, Y., Hao, F., 2014. Vertical and horizontal

510   distribution of soil parameters in intensive agricultural zone and effect on diffuse

511   nitrogen pollution. Soil & Tillage Research 144, 32-40.

512   Ju, X.T., Gu, B.J., Wu, Y.Y., Galloway, J.N., 2016. Reducing China's fertilizer use by

513   increasing farm size. Global Environmental Change 41, 26-32.

514   Liu, W.F., Yang, H., Liu, J.G., Azevedo, L.B., Wang, X.Y., Xu, Z.X., Abbaspour, K.C.,

515   Schulin, R., 2016. Global assessment of nitrogen losses and trade-offs with yields

516   from major crop cultivations. Science of the Total Environment 572, 526-537.

517   Raupach, M. R., Marland, G., Ciais, P., Le Quéré, C., Canadell, J. G., Klepper, G., Field,

518   C. B., 2007. Global and regional drivers of accelerating CO_2 emissions.

519   Proceedings of the National Academy of Sciences 104, 10288-10293.

520 Korsaeth, A., Eltun, R., 2000. Nitrogen mass balances in conventional, integrated and

521   ecological cropping systems and the relationship between balance calculations and

522   nitrogen runoff in an 8-year field experiment in Norway. Agriculture, Ecosystems

523   & Environment 79, 199-214.

524 Leip, A., Britz, W., Weiss, F., de Vries, W., 2011. Farm, land, and soil nitrogen budgets

525   for agriculture in Europe calculated with CAPRI. Environmental Pollution 159,

526   3243-3253.

527 Liang, X.Q., Tian, G.M., Li, H., Chen, Y.X., Zhu, S., 2005. Study on characteristic of

528   nitrogen and phosphorus loss from rice field by natural rainfall runoff. Journal of

529   Soil Water Conservation 19, 59-63.

530 Liu, J.G., You, L.Z., Amini, M., Obersteiner, M., Herrero, M., Zehnder, A.J.B., Yang,

531   H., 2010. A high-resolution assessment on global nitrogen flows in cropland.

532   Proceedings of the National Academy of Sciences 107, 8035-8040.

533 Liu, Q., Li, Z.B., Li, P., 2014. Effect of runoff dynamic on sediment and nitrogen losses

534   in an agricultural watershed of the southern Shaanxi region, China. Clean-Soil Air

535   Water 42, 56-63.

536 Miyazato, T., Mohammed, R.A., Lazaro, R.C., 2010. Irrigation management transfer

537   (IMT) and system of rice intensification (SRI) practice in the Philippines. Paddy

538   and Water Environment 8, 91-97.

539   Mueller, N. D., Gerber, J. S., Johnston, M., Ray, D. K., Ramankutty, N., & Foley, J. A.

540   2012. Closing yield gaps through nutrient and water management. Nature, 490,

541   254-257.

542   Paerl, H.W., Hall, N.S., Peierls, B.L., Rossignol, K.L., 2014. Evolving paradigms and

543   challenges in estuarine and coastal eutrophication dynamics in a culturally and

544   climatically stressed world. Estuaries and Coasts 37, 243-258.

545   Piao, S., Yin, G., Tan, J., Cheng, L., Huang, M., Li, Y., Liu, R., Mao, J., Myneni, R.B.,

546   Peng, S., Poulter, B., Shi, X., Xiao, Z., Zeng, N., Zeng, Z., Wang, Y., 2015.

547   Detection and attribution of vegetation greening trend in China over the last 30

548   years. Global Change Biology 21, 1601-1609.

549   Rasouli, S., Whalen, J.K., Madramootoo, C.A., 2014. Review: reducing residual soil

550   nitrogen losses from agroecosystems for surface water protection in Quebec and

551   Ontario, Canada: best management practices, policies and perspectives. Canadian

552   Journal of Soil Science 94, 109-127.

553   Raymond, P.A., David, M.B., Saiers, J.E., 2012. The impact of fertilization and

554   hydrology on nitrate fluxes from Mississippi watersheds. Current Opinion in

555   Environmental Sustainability 4, 212-218.

556   Seitzinger, S.P., Mayorga, E., Bouwman, A.F., Kroeze, C., Beusen, A.H.W., Billen, G.,

557   Van Drecht, G., Dumont, E., Fekete, B.M., Garnier, J., Harrison, J.A., 2010. Global

558   river nutrient export: A scenario analysis of past and future trends. Global

559   Biogeochemical Cycles 24, 2621-2628.

560 Schaefer, S.C., Alber, M., 2007. Temperature controls a latitudinal gradient in the

561   proportion of watershed nitrogen exported to coastal ecosystems. Biogeochemistry

562   85, 333-346.

563 SEPA, 2002. Standard methods for the examination of water and wastewater version 4.

564   Beijing: China Environmental Science Press.

565 Shen, Z.Y., Liao, Q., Hong, Q., Gong, Y.W., 2012. An overview of research on

566   agricultural non-point source pollution modelling in China. Separation and

567   Purification Technology 84, 104-111.

568 Shi, L.H., Ji, X.H., Li, H.S., Tian, F.X., Peng, H., Liu, S.B., 2010. Nitrogen and

569   phosphorus losses from surface runoff under different application in the double

570   cropping rice fields in Hunan (in Chinese). Chinese Journal of Agrometeorology

571   31, 551-557.

572 Sobota, D.J., Harrison, J.A., Dahlgren, R.A., 2009. Influences of climate, hydrology,

573   and land use on input and export of nitrogen in California watersheds.

574   Biogeochemistry 94, 43-62.

575 Sorooshian, S., AghaKouchak, A., Li, J.L., 2014. Influence of irrigation on land

576   hydrological processes over California. Journal of Geophysical Research-

577   Atmospheres 119, 13137-13152.

578 Stalnacke, P., Pengerud, A., Vassiljev, A., Smedberg, E., Morth, C.M., Hagg, H.E.,

579   Humborg, C., Andersen, H.E., 2015. Nitrogen surface water retention in the Baltic

580   Sea drainage basin. Hydrology and Earth System Sciences 19, 981-996.

581   Streimikiene, D., Balezentis, T., 2016. Kaya identity for analysis of the main drivers of

582   GHG emissions and feasibility to implement EU "20-20-20" targets in the Baltic

583   States. Renewable & Sustainable Energy Reviews 58, 1108-1113.

584   Ti, C.P., Yan, X.Y., 2013. Spatial and temporal variations of river nitrogen exports from

585   major basins in China. Environmental Science and Pollution Research 20, 6509-

586   6520.

587   Tilman, D., Balzer, C., Hill, J., Befort, B.L., 2011. Global food demand and the

588   sustainable intensification of agriculture. Proceedings of the National Academy of

589   Sciences, USA 108, 20260-20264.

590   Van Damme, M.; Whitburn, S.; Clarisse, L.; Clerbaux, C.; Hurtmans, D.; Coheur, P. F.

591   Version 2 of the IASI NH3 neural network retrieval algorithm; near-real time and

592   reanalysed datasets. Atmos. Meas. Technol. Disc. 2017,, doi:110.5194/amt-2017-

593   239

594   Velthof, G.L., Oudendag, D., Witzke, H.P., Asman, W.A., Klimont, Z., Oenema, O.,

595   2009. Integrated assessment of nitrogen losses from agriculture in EU-27 using

596   MITERRA-EUROPE. Journal of Environmental Quality 38, 402-417.

597   Wäldchen, J., Schoning, I., Mund, M., Schrumpf, M., Bock, S., Herold, N., Totsche,

598   K.U., Schulze, E.D., 2012. Estimation of clay content from easily measurable water

599   content of air-dried soil. Journal of Plant Nutrition and Soil Science 175, 367-376.

600   Wang, J., Lu, G.A., Guo, X.S., Wang, Y.Q., Ding, S.W., Wang, D.Z., 2015a.

601   Conservation tillage and optimized fertilization reduce winter runoff losses of

602   nitrogen and phosphorus from farmland in the Chaohu Lake region, China.

603   Nutrient Cycling in Agroecosystems 101, 93-106.

604   Wang, S., Fu, B., Piao, S., Lü, Y., Ciais, P., Feng, X., Wang, Y., 2015b. Reduced

605   sediment transport in the Yellow River due to anthropogenic changes. Nature

606   Geoscience 9, 38-41.

607   Wang, X.L., Feng, A.P., Wang, Q., Wu, C.Q., Liu, Z., Ma, Z.S., Wei, X.F., 2014. Spatial

608   variability of the nutrient balance and related NPSP risk analysis for agro-

609   ecosystems in China in 2010. Agriculture, Ecosystems & Environment 193, 42-52.

610   Wu, L., Tang, S.R., He, D.D., Wu, X., Shaaban, M., Wang, M.L., Zhao, J.S., Khan, I.,

611   Zheng, X.H., Hu, R.G., Horwath, W.R., 2017. Conversion from rice to vegetable

612   production increases N_2O emission via increased soil organic matter mineralization.

613   Science of the Total Environment 583, 190-201.

614   Xu, J., Shan, L.N., Yu, D.P., Li, Z.L., He, Y.F., 2013. Effects of different fertilization

615   modes on nitrogen use efficiency of cabbages and nitrogen loss from vegetable

616   field (in Chinese). Journal of Zhejiang University 39, 556-564.

617   Yan, R., Gao, J., Huang, J., 2016. WALRUS-paddy model for simulating the

618   hydrological processes of lowland polders with paddy fields and pumping stations.

619   Agricultural Water Management 169, 148-161.

620   Yan, X., Ti, C., Vitousek, P., Chen, D., Leip, A., Cai, Z., Zhu, Z., 2014. Fertilizer

621   nitrogen recovery efficiencies in crop production systems of China with and

622   without consideration of the residual effect of nitrogen. Environmental Research

623   Letters 9, 095002.

624   Yang, S.H., Peng, S.Z., Xu, J.Z., He, Y.P., Wang, Y.J., 2015. Effects of water saving

625   irrigation and controlled release nitrogen fertilizer managements on nitrogen losses

626   from paddy fields. Paddy and Water Environment 13, 71-80.

627   Yu, Q.G., Ye, J., Ma, J.W., Sun, W.C., Wang, Q., Jiang, L.N., Fu, J.R., Chen, Y., 2011.

628   Effects of different nitrogen applied levels on nitrogen runoff loss in oilseed rape

629   fields (in Chinese). Journal of Soil and Water Conservation 25, 22-25.

630   Zhang, X., Davidson, E.A., Mauzerall, D.L., Searchinger, T.D., Dumas, P., Shen, Y.,

631   2015. Managing nitrogen for sustainable development. Nature 528, 51-59.

632   Zhang, Y., Zhou, Y., Shao, Q., Liu, H., Lei, Q., Zhai, X., Wang, X., 2016. Diffuse

633   nutrient losses and the impact factors determining their regional differences in four

634   catchments from North to South China. Journal of Hydrology 543, 577-594.

635   Zheng, D., Hunt Jr., E.R. and Running, S.W. 1993. A daily soil temperature model based

636   on air temperature and precipitation for continental applications. Climate Research,

637   2, 183-191..

638   Zhou, F., Shang, Z., Zeng, Z., Piao, S., Ciais, P., Raymond, P.A., Wang, X., Wang, R.,

639   Chen, M., Yang, C., Tao, S., Zhao, Y., Meng, Q., Gao, S., Mao, Q., 2015. New

640   model for capturing the variations of fertilizer-induced emission factors of N_2O.

641   Global Biogeochemical Cycles 29, 885-897.